

BALCI, M., DOKUR, E., YUZGEC, U. and ERDOGAN, N. 2024. Multiple decomposition-aided long short-term memory network for enhanced short-term wind power forecasting. *IET renewable power generation* [online], 18(3), pages 331-347. Available from: <https://doi.org/10.1049/rpg2.12919>

Multiple decomposition-aided long short-term memory network for enhanced short-term wind power forecasting.

BALCI, M., DOKUR, E., YUZGEC, U. and ERDOGAN, N.

2024

ORIGINAL RESEARCH

Multiple decomposition-aided long short-term memory network for enhanced short-term wind power forecasting

Mehmet Balci¹  | Emrah Dokur²  | Ugur Yuzgec³  | Nuh Erdogan⁴ 

¹Graduate Education Institute, Bilecik Seyh Edebali University, Bilecik, Türkiye

²Department of Electrical Electronics Engineering, Bilecik Seyh Edebali University, Bilecik, Türkiye

³Department of Computer Engineering, Bilecik Seyh Edebali University, Bilecik, Türkiye

⁴Department of Engineering, School of Science and Technology, Nottingham Trent University, Nottingham, UK

Correspondence

Mehmet Balci, Graduate Education Institute, Bilecik Seyh Edebali University, Bilecik 11000, Türkiye.
Email: mehmet.balci@bilecik.edu.tr

Abstract

With the increasing penetration of grid-scale wind energy systems, accurate wind power forecasting is critical to optimizing their integration into the power system, ensuring operational reliability, and enabling efficient system asset utilization. Addressing this challenge, this study proposes a novel forecasting model that combines the long-short-term memory (LSTM) neural network with two signal decomposition techniques. The EMD technique effectively extracts stable, stationary, and regular patterns from the original wind power signal, while the VMD technique tackles the most challenging high-frequency component. A deep learning-based forecasting model, i.e. the LSTM neural network, is used to take advantage of its ability to learn from longer sequences of data and its robustness to noise and outliers. The developed model is evaluated against LSTM models employing various decomposition methods using real wind power data from three distinct offshore wind farms. It is shown that the two-stage decomposition significantly enhances forecasting accuracy, with the proposed model achieving R^2 values up to 9.5% higher than those obtained using standard LSTM models.

1 | INTRODUCTION

Wind energy has emerged as the leading form of renewable energy in the global effort to decarbonize energy production and achieve net-zero targets [1]. Its widespread adoption has been instrumental in reducing emissions and transitioning towards a more sustainable energy future. As of 2023, the global installed capacity of wind power has reached 906 GW [2]. The increasing penetration of wind energy systems has raised concerns about their power grid integration, such as stability and reliability [3]. This is primarily due to the intermittency and randomness of the wind in nature. Therefore, accurate wind power forecasting is essential for maintaining a reliable and safe power system [4].

Forecasting methods can be broadly categorized into four types: physical, statistical, artificial intelligence (AI), and hybrid methods. Physical methods utilize meteorological data and mathematical models to predict wind power, taking into account factors such as temperature, humidity, pressure, and other relevant meteorological variables [5]. Statistical methods often use historical data to extract fluctuations and regularities [6]. Sta-

tistical methods can employ either the moving average method over a particular period or advanced statistical techniques such as regression analysis. The well-known conventional statistical models are the auto-regressive moving average (ARMA) [7], auto-regressive integrated moving average (ARIMA) [8], and seasonal-ARIMA (SARIMA) models [9]. The use of artificial intelligence (AI) models in wind power forecasting has become increasingly prevalent with the advancement of computer science and technology. Various AI-based models such as artificial neural networks [10], extreme learning machine [11], fuzzy logic models [12], and support vector machines [13] have been successfully applied. Among these models, deep learning has gained significant attention in wind power forecasting due to its feature extraction and nonlinear fitting capabilities [14, 15]. Lastly, the hybrid methods have been proposed to further improve forecasting accuracy by combining AI-based models with models that use meta-heuristic algorithms, such as the Dragonfly algorithm and the grey wolf optimizer [16, 17].

Signal decomposition methods play a crucial role in enhancing the accuracy of wind power forecasting in hybrid models. These methods enable a more detailed analysis of the wind

This is an open access article under the terms of the [Creative Commons Attribution](https://creativecommons.org/licenses/by/4.0/) License, which permits use, distribution and reproduction in any medium, provided the original work is properly cited.

© 2023 The Authors. *IET Renewable Power Generation* published by John Wiley & Sons Ltd on behalf of The Institution of Engineering and Technology.

signal by decomposing a wind time-series signal into distinct components with varying frequencies. A common decomposition technique is empirical mode decomposition (EMD), which uses a data-driven approach to decompose the wind signal into a set of intrinsic mode functions (IMFs) that capture the different time scales of the wind signal [18]. Another decomposition method is the singular spectrum analysis (SSA) which decomposes the wind signal into a set of orthogonal components that represent different temporal patterns in the wind signal [19]. In [20], the seasonal decomposition of time series (STL) method is proposed to decompose a time series into three components: the trend, the seasonal, and the residual components. It is shown to be effective in identifying long-term trends and repeating patterns in the data [20]. Wavelet decomposition (WD) method, on the other hand, decomposes a wind signal into different frequency bands using the wavelet transform. It can be used to identify patterns in the wind signal that occur at different frequencies [21]. The swarm decomposition method (SWD) is another signal processing technique for the analysis of non-stationary signals. The method utilizes a swarm filtering approach that is based on the swarm-prey hunting analogy to decompose a signal into a series of generated oscillating components [22]. The resulting components are considered to be the original signal and are used to describe the behaviour of the signal at different frequencies [23]. Numerous studies in the literature integrated various decomposition techniques into machine learning models such as multi-layer perceptron (MLP), adaptive neuro-fuzzy inference system (ANFIS), extreme learning machine (ELM), and long short term memory (LSTM) to improve their forecasting performance. Multiple decomposition approaches have demonstrated enhanced stability and efficacy in wind power forecasting. Table 1 presents an overview of forecasting models incorporating multiple decompositions in the context of wind energy studies. To enhance the linearity and stability of wind speed characteristics, it is possible to employ a combination of multiple decomposition techniques [24]. While each method has its own benefits and drawbacks, the selection of a particular method depends on the unique characteristics of the wind signal and the objectives of the analysis. While models utilizing a single decomposition technique exhibit superior performance compared to their non-decomposed counterparts, they are susceptible to overfitting and local minima weaknesses. Models with multiple decomposition steps, in particular those extracting additional features for high-frequency components, can yield enhanced forecasting accuracy. Given the characteristics of randomness, fluctuation, nonlinearity, and uncertainty in wind data, decomposing it into multiple components can help better characterize these features in forecasting models. Among various data processing methods, the variational mode decomposition (VMD) algorithm stands out by effectively separating wind speed into distinct components fluctuating around a central frequency. This approach facilitates the extraction of the nonlinear, linear, and noise components of wind speed, contributing to a more detailed representation of the data. In contrast, the mode decomposition (EMD) method is an adaptive data processing method that can handle non-linear and non-stationary time series. However, EMD is not with-

out its drawbacks, such as mode mixing problems. To address some limitations, the VMD algorithm emerges as a promising solution, mitigating the issues introduced by the EMD method and enhancing the overall efficacy of the decomposition process. In particular, decomposing the highest frequency component using VMD further elevates the performance of the forecasting model. The proposed combination supports the strengths of each decomposition technique, thereby providing a more robust and accurate wind power forecasting solution.

In [25], a hybrid wind speed forecasting model is proposed by combining EMD with a regularized version of the adaptive neuro-fuzzy inference system (ELANFIS). The regularized ELANFIS with the EMD is then used to forecast the wind speed by learning a nonlinear representation of the IMFs. It is shown that the proposed model displayed superior as compared to the single ELANFIS model [25]. In [26], a new wind speed forecasting approach combines artificial neural network based model with fast ensemble empirical mode decomposition (EEMD). The model parameters are also optimized using genetic algorithm (GA) and mind evolutionary algorithm (MEA). A multi-step deep learning-based wind speed forecasting model is presented in [27]. The model integrates several signal processing techniques such as variational mode decomposition (VMD), singular spectrum analysis (SSA) into long short-term memory (LSTM) network and extreme learning machine (ELM) based models. The LSTM network is used to model the temporal dependencies of the IMFs, while the ELM is then employed to improve forecasting accuracy by learning a nonlinear representation of the IMFs. It is shown that the proposed model improved the forecasting accuracy compared to using a single LSTM or ELM model.

Decomposition methods for wind power forecasting have several limitations. They are sensitive to noise in the wind signal, which can lead to incorrect IMFs being extracted and inaccurate wind predictions. Moreover, they may not be able to extract all the IMFs correctly, which can lead to some patterns in the wind signal being missed. This can affect the accuracy of wind power forecasting, as important patterns in the wind signal may not be captured. To overcome these limitations, this study proposes using a secondary decomposition method to extract IMFs that are more accurate, less affected by noise, and capture additional patterns in the wind signal. By combining these different patterns that lead to a more comprehensive analysis of the wind signal, each component can be forecasted more effectively. The proposed EMD-VMD-LSTM model employs the empirical mode decomposition (EMD) method to decompose the wind power signal into intrinsic mode functions (IMFs). The variational mode decomposition (VMD) method is then applied to the highest IMF as a secondary decomposition step. All the decomposed signals are then used to train LSTM network. LSTM networks are a type of recurrent neural network (RNN) that are well-suited for modelling sequential data, such as wind power data, due to its ability to remember past information and update the hidden state at each time step. In this respect, the main salient contributions of this study can be summarized as follows:

TABLE 1 Overview of the studies on secondary decomposition for wind forecasting.

Reference	Method	Dataset	Application
Jiang et al. (2023) [28]	SD-MLXGBoost-GA-GRU (Secondary Decomposition - multi-label specific XGBoost - genetic algorithm - convolutional gated recurrent unit network)	Wind speeds measured 10-min interval from wind farm in Shandong Province, China	Wind forecasting for 1-step, 6-step and 10-step ahead
Wang et al. (2023) [29]	Complete ensemble empirical mode decomposition with adaptive noise (CEEMDAN), singular-spectrum analysis (SSA), elastic neural network, extreme gradient boosting (Xgboost) and Gaussian process (GP) are used	Wind speed of four places in Gansu, China	Wind speed forecasting
Liu et al. (2023) [30]	STL-OVMD-LSTM (seasonal-trend decomposition - optimal variational mode decomposition - long short-term memory)	Wind direction for a whole year 10-min interval	One, three and five step wind direction prediction
Zhai and Li (2022) [31]	EMD-VMD-PSO-ELM (EMD-VMD - particle swarm optimization - extreme learning machine)	Measure wind speed 1-min interval from National Wind Speed Observatory of the US	Short-term wind speed forecasting
Emeksiz and Tan (2022) [32]	CEEMDAN- LMD-Hurst-BPNN (comprised of ensemble empirical mode decomposition adaptive noise - local mean decomposition - Hurst and back-propagation neural network)	10-min interval measured wind speed from Tokat Gaziosmanpasa University Campus	Forecasting of short and medium term wind speed
R.G. Silva et al. (2022) [33]	VMD-SSA-STACK (VMD- singular spectrum analysis - stacking-ensemble learning)	Wind speed measurement 10-min intervals in the State of Rio Grande do Norte, Brazil	Wind speed prediction for 10-min, 30-min, 60-min ahead
Sibtain et al. (2022) [34]	Three-layered structure utilizing VMD, improved complete ensemble empirical mode decomposition with additive noise (ICEEMDAN), and a LSTM	10-min interval wind speed from the Shahabad wind mast at Sujawal, Pakistan	Ultrashort term wind speed forecasting (10-min)
Zhang et al. (2022) [35]	EWP-CS-RELM (ensemble empirical mode decomposition (EEMD) and wavelet packet transform (WPT) - Cuckoo search - regularized extreme learning machine)	Wind speeds measured 15-min intervals from two wind farms in Shandong Province, China	One,three, five steps ahead wind speed prediction
Goh et al. (2022) [36]	CEEMDAN-VMD-ELM-CNN-BiLSTM (CEEMDAN-VMD-ELM - convolutional neural networks - bidirectional long short-term memory)	Measured wind speed 10-min interval in La Haute Borne, France	Short-term wind speed prediction one to three step
Sun et al. (2021) [37]	WT-VMD-RF-K-means-LSTM-LSTM (wavelet transform, variational mode decomposition, random forest, K-means and LSTM)	Measured wind power 10-min two wind farms of Hebei Province in China	Forecasting wind power 15-min to 1-h ahead
Sun et al. (2021) [38]	VMD-SGMD-DE-BP (variational mode decomposition - symplectic geometry mode decomposition - differential evolution - back propagation)	Four datasets of 20-min interval wind speed in Chengde, China	Forecasting wind speed by four steps ahead
Zhang et al. (2021) [39]	SSA-MEMD-ACNN-BiLSTM (singular spectrum analysis - multivariate EMD - CNN optimized via the attention mechanism - BiLSTM)	1-h measured four wind speed datasets from Texas and California	Wind speed forecasting (under 1-h)
Wu et al. (2020) [40]	VMD-EMD (variational mode decomposition - empirical mode decomposition) and VMD-EWT (VMD - empirical wavelet transform) based forecasting models	Eight datasets measured 15-min interval in Elia, Belgium	Wind power forecasting by three steps ahead

(Continues)

TABLE 1 (Continued)

Reference	Method	Dataset	Application
Xiang et al. (2020) [41]	SD-BiGRU-CSO(FIG) (secondary decomposition - bidirectional gated recurrent unit - chicken swarm optimization/fuzzy information granule)	Wind speeds measured 10-min interval from Zhejiang and Hubei	1-h wind speed forecasting
Wu and Xiao (2019) [42]	SD-AL-WNN (secondary decomposition - active learning - wavelet neural network)	Four different wind speed datasets collected from Ontario Province, Canada	Forecasting wind speed and direction
Liu et al. (2019) [43]	EEMD-SE-WPD-BGA-GMDH (ensemble empirical mode decomposition - sample entropy - wavelet packet decomposition - binary-coded genetic algorithm - group method of data handling)	20-min interval wind speed from three different wind turbines of Hami wind farm, Xinjiang Province, China	1-step to 6-step (20-min to 120-min) ahead wind speed prediction
Zhang et al. (2019) [44]	VMD-WT-PCA-BP-RBF (VMD - wavelet transform - principal component analysis-back propagation screening - radial basis function)	Measured 10-min intervals from Sotavento wind farm in Spain and the Changma wind farm in China	Predict wind speed 10-min ahead
Liu et al. (2018) [45]	WD-SampEn-VMD-MadaBoost-BFGS-WF (wavelet decomposition - sample entropy - variational mode decomposition - modified AdaBoost.RT - Broyden-Fletcher-Goldfarb-Shanno quasi-Newton back propagation - wavelet filter)	Simulated wind speeds	Forecasting wind speed

- To effectively analyze and model the complex dynamics of wind power data, a robust multi-decomposition process employing EMD and VMD is proposed.
- By taking advantage of its robustness to noise and data outliers, the LSTM is developed to exploit the learning features of nonlinear wind power data. As such, the forecasting performance is maximized.
- The robustness of the proposed model is tested on multivariate offshore wind farm (OWF) data with different characteristics from three different regions. Its performance is assessed through LSTM variants and error metrics. By identifying significant variables in OWF data and subseries from the multiple decomposition, the proposed model provides valuable insights for wind power forecasting, aiding decision-making.

The remainder of the paper is organized as follows: Section 2 describes the principles of the signal decomposition techniques and the LSTM model, and presents the characteristics of the collected wind data. Section 3 presents the forecasting results and a comparative analysis of the different models. Section 4 provides concluding remarks.

2 | MATERIALS AND METHODS

This study proposes a multiple decomposition approach to enhance the forecasting performance of a deep learning model, i.e. the LSTM network, for wind power forecasting. The methodology first employs the EMD to decompose the original wind power signal into IMFs that represent different frequency components. The VMD is then applied to the highest-frequency

IMF to further decompose it into a set of subcomponents with more localized frequency and amplitude characteristics. This two-stage decomposition process effectively extracts hidden patterns and reduces noise from wind power data, thereby enhancing the forecasting performance of the LSTM model. The LSTM network is then trained using all the decomposed signals to capture the complex relationships and non-linear patterns inherent in wind power data. The equations for each model step are described in the following subsections. The collected OWF dataset to test the model is also described in a separate subsection below.

2.1 | EMD (empirical mode decomposition)

Empirical mode decomposition (EMD) is a technique for analyzing and decomposing signals into a set of intrinsic mode functions (IMFs) and residual components. It is based on that a signal can be represented as a sum of oscillatory components of different frequencies and amplitudes, i.e. IMFs [46]. The IMFs are defined as the functions that, when added together, reconstruct the original signal, and that have zero mean, similar extrema, and similar mean value. EMD is a data-driven method that does not rely on any assumptions about the underlying signal or the properties of the IMFs, making it well-suited for non-linear and non-stationary signals. It has been widely used in various fields such as biomedical signal processing, image processing, and time series analysis.

The EMD decomposes a given signal iteratively into a series of IMFs and a residual component. With the EMD algorithm, the data is divided into non-overlapping time scale components and signal oscillations are considered locally. It decomposes $x(t)$

signal into intrinsic mode functions (IMF) with an endpoint between two consecutive zero-crossing points and an average value of zero. If data set $x(t)$, IMFs $x_n(t)$ and a residuum $r(t)$, the signal is [47];

$$x(t) = \sum_n x_n(t) + r(t) \quad (1)$$

The steps for using the EMD are as follows.

1. Beginning values; $n = 1, r_0(t) = x(t)$
2. If the n th IMF comes out:
 - i. Adjust $b_0(t) := r_{n-1}(t)$ and $k := 1$
 - ii. Define whole local minima and maxima of $b_{k-1}(t)$
 - iii. Envelop $U_{k-1}(t)$ with maximums and envelope $L_{k-1}(t)$ with minimums are defined for $b_{k-1}(t)$
 - iv. The average of both envelopes of $r_{k-1}(t)$ is determined; $m_{k-1}(t) = \frac{1}{2}(U_{k-1}(t) + L_{k-1}(t))$
 - v. k th component is created; $b_k(t) := b_{k-1}(t) - m_{k-1}(t)$
 - a. if b_k is not eligible for all IMF requirements, k is incremented by one ($k + 1$) and the operations are repeated starting from step [ii]
 - b. if b_k qualifies for IMF requirements $x_n(t) := b_k(t)$ and $r_n(t) := r_{n-1}(t) - x_n(t)$
3. If r_n creates a residue, the process is terminated, if not, n is incremented by one ($n + 1$) and the processes are repeated from step one.

2.2 | VMD (variational mode decomposition)

The VMD is a signal processing technique used to decompose a signal into a sum of IMFs, which are oscillatory components with distinct frequency and time characteristics. VMD is an extension of the traditional empirical mode decomposition (EMD) method, which is based on the local maxima and minima of a signal [48].

The main advantage of the VMD over the EMD is that it can deconstruct non-stationary and nonlinear signals, which can be difficult to decompose with the EMD. The VMD also allows control of the number of IMFs generated, which can help to reduce computational complexity and focus on specific frequency components of a signal [49].

The mathematical structure of the VMD can be represented as [50]:

$$x(t) = \sum_{k=1}^K u_k(t) \quad (2)$$

The bandwidth of $u_k(t)$ signals is considered narrow in the frequency space. The cost function of problem can be given by [51];

$$\arg \min_{u_k, w_k, \lambda} \alpha \sum_{k=1}^K \left\| \partial_t \left[\left(\sigma(t) + \frac{j}{\pi t} \right) \times u_k(t) \right] e^{-jw_k t} \right\|_2^2 + \|\lambda\|_2^2 - \sum u_k \|\lambda\|_2^2 + \left\langle \lambda, r - \sum u_k \right\rangle \quad (3)$$

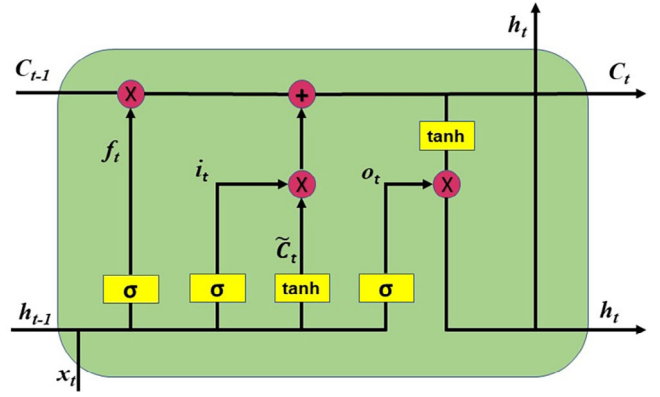


FIGURE 1 The architecture of an LSTM.

which is solved for each (w_k, s_k) using alternating direction method of multipliers.

2.3 | Long-short term memory (LSTM) model

Long short-term memory (LSTM) is a type of recurrent neural network (RNN) that can retain long-term dependencies in sequential data. It is specifically designed to avoid the vanishing gradient problem, which is a common issue in traditional RNNs, making it difficult to learn long-term dependencies. LSTMs are composed of a series of “cells” that process and transmit information, and each cell contains three types of gates: input, forget, and output gates. These gates allow the LSTM to selectively retain or discard information from the previous time steps, which allows it to learn and maintain long-term dependencies [52]. Figure 1 shows the general structure of the LSTM.

The following steps are used to calculate the output of LSTM [53];

1. The x_t and h_{t-1} values are obtained and the value to be thrown is determined with a f_t sigmoid function.

$$f_t = \sigma(\omega_f \cdot [h_{t-1}, x_t] + b_f) \quad (4)$$

2. The information to be stored is decided by a sigmoid layer. A new candidate value \tilde{C}_t ; calculated with x_t, h_{t-1} and $\tanh(\cdot)$.

$$i_t = \sigma(w_i \cdot [h_{t-1}, x_t] + b_i) \quad (5)$$

$$\tilde{C}_t = \tanh(w_c \cdot [h_{t-1}, x_t] + b_c) \quad (6)$$

3. New C_t status is calculated by multiplying i_t by \tilde{C}_t and adding it to the previous term as follows:

$$C_t = f_t \times C_{t-1} + i_t \times \tilde{C}_t \quad (7)$$

4. Output information is decided by the sigmoid layer.

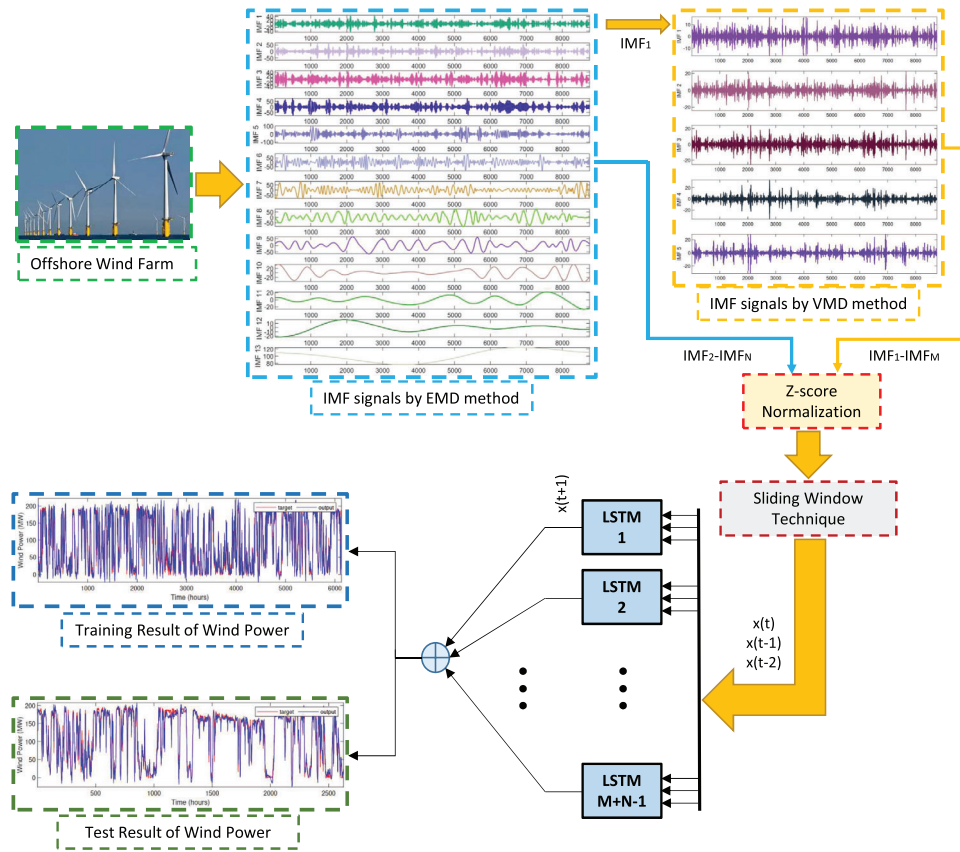


FIGURE 2 The architecture of the proposed EVL model.

$$s_t = \sigma(w_0 \cdot [b_{t-1}, x_t] + b_0) \quad (8)$$

$$b_t = s_t \times \tanh(C_t) \quad (9)$$

2.4 | The EVL (EMD-VMD-LSTM) model

The proposed EVL model can effectively capture the complex and nonlinear characteristics of wind power time series data, as it combines the advantages of three different methods. The architecture of EVL model is depicted in Figure 2.

The EMD method extracts the IMFs of the wind power data, which represent the various frequency components and provide a better understanding of the underlying data structure. The VMD method further decomposes the highest-frequency IMF, providing more detailed information about the oscillation modes with different time-frequency properties. By using LSTM models to forecast each IMF one step ahead, the EVL model provides accurate and reliable predictions for short-term wind power. Overall, this approach can improve forecasting accuracy and support decision-making in the wind power industry. The proposed EVL model consists of four steps:

1. Using EMD method, the wind power data is separated into IMFs with different frequencies.
2. The highest-frequency component of the IMFs obtained by the EMD is decomposed, is deconstructed using the

VMD method to obtain new IMFs that replace the highest-frequency component. This step is taken to address the potential negative impact of the highest-frequency component on the forecasting accuracy.

3. The decomposed signals of wind power data are then divided into training and test sets with a ratio of 70% to 30%, respectively. The IMFs obtained with both decomposition methods are processed using the LSTM model to forecast the short-term wind power. Each decomposed signal is utilized as an input to the LSTM model independently, hence the EVL comprises of an LSTM model for each decomposed signal. The total number of LSTM models used in the model is $M + N - 1$, where N is the number of decomposed signals obtained from the primary decomposition with the EMD and M is the number of decomposed signals obtained from the secondary decomposition of the highest frequency IMF with the VMD. The sliding window technique is used to train the developed model, with a window size of three. The decomposed signals are fed to the LSTM models to forecast the value of each decomposed signal for the next step.
4. The forecasted values of the decomposed components are aggregated to find the wind power forecasted value. Z-score normalization is used for the training stage, and the same hyperparameters are preferred for all LSTM models. After the training stage of the LSTM models, the test results are obtained using 30% of the data set.

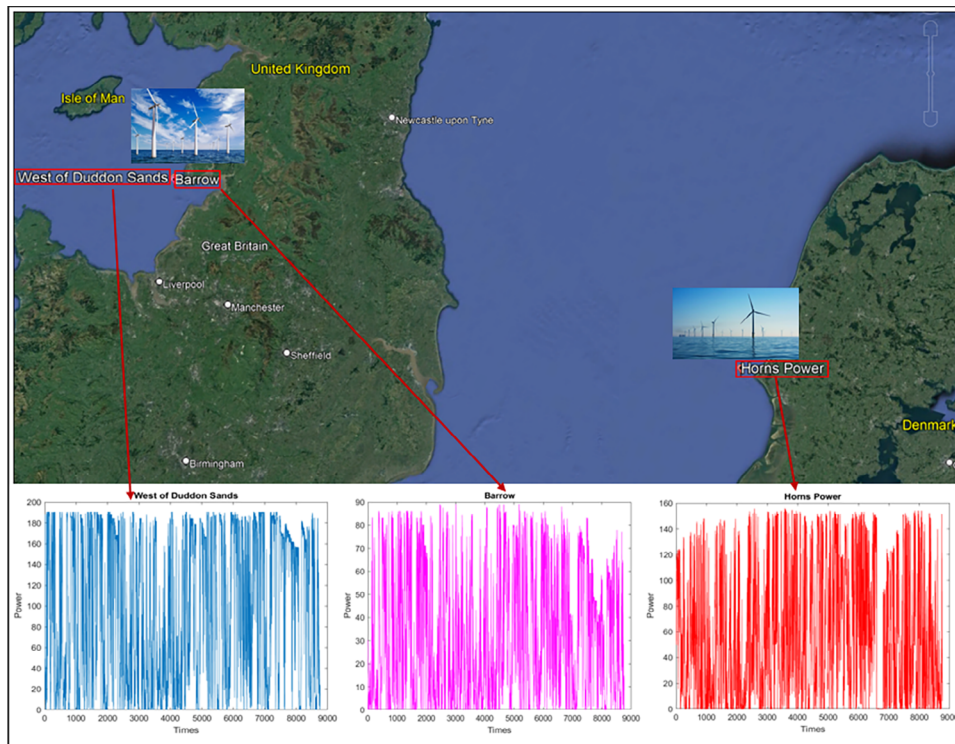


FIGURE 3 Locations of offshore wind farms for the collected data.

2.5 | Offshore wind power dataset

The performance of the proposed model is tested using a real wind power dataset. The data includes 1 year of wind power data measurements in a 1-h time interval from three OWFs, i.e. West of Duddon Sands, Barrow, and Horns Power. As such, each data set has a vector of 8760 wind power measurements. The locations of the OWFs are shown in Figure 3. The key characteristics of the OWFs can be summarized as follows: West of Duddon Sands OWF has an installed capacity of 388.8 MW, utilizing 108 Siemens SWT-3.6-120 turbines with an 80.0-m hub height. Barrow OWF has an installed capacity of 90.0 MW, utilizing 30 Vestas V90-3000 offshore turbines with a 75.0-m hub height. Horns Power OWF has an installed capacity of 160 MW, utilizing 49 Vestas V80-2000 turbines with a 70.0-m hub height. The standard deviations of their datasets are 72.0836, 51.1955, and 28.1497 for the West of Duddon Sands, Horns Power, and Barrow OWFS, respectively.

3 | RESULTS AND DISCUSSION

To assess the impact of the proposed multiple decomposition on the forecasting performance, a comparative analysis was conducted against the LSTM models. This first LSTM model did not include any decomposition technique to display its performance to be used as benchmarking. The second model included the EMD as a single decomposition technique to demonstrate the impact of the EMD. The other two models employed

multiple decomposition techniques to assess how the EMD behaviour changed with the SWD and WD techniques. As such, the impact of the VMD on forecasting performance could be assessed by capturing the complex and nonlinear characteristics of wind power time series data.

The proposed EVL model was implemented and evaluated using MATLAB 2020b on a personal computer equipped with an Intel Core i5-7500 Microprocessor with a clock speed of 3.40 GHz, a 128 MB Intel HD Graphics 630 graphics card, and 16 GB of RAM. Each LSTM used in this model has the same hyperparameters and it was trained for 10 epoch using a batch size of 10 and an initial learning rate of 0.005. A dropout value of 0.5 was employed to prevent overfitting. The optimization algorithm used was Adam, and the LSTM model consists of 2 hidden layers with 100 neurons each.

The first step of the EVL model involved the application of the EMD decomposition method to the wind power dataset in the pre-processing phase. Figure 4 shows the IMF signals decomposed by EMD method for West of Duddon Sands OWF dataset. As shown in this figure, the EMD method resulted in the generation of a total of 13 IMFs for the West of Duddon Sands dataset. These IMFs represent the different intrinsic oscillatory patterns present in the original signals and provide a more detailed and interpretable representation of the data.

In the second pre-processing stage of the model, the secondary decomposition method (e.g. VMD) was applied to the highest-frequency IMF signal (IMF1) decomposed by EMD method. Figure 5 depicts the results of the secondary

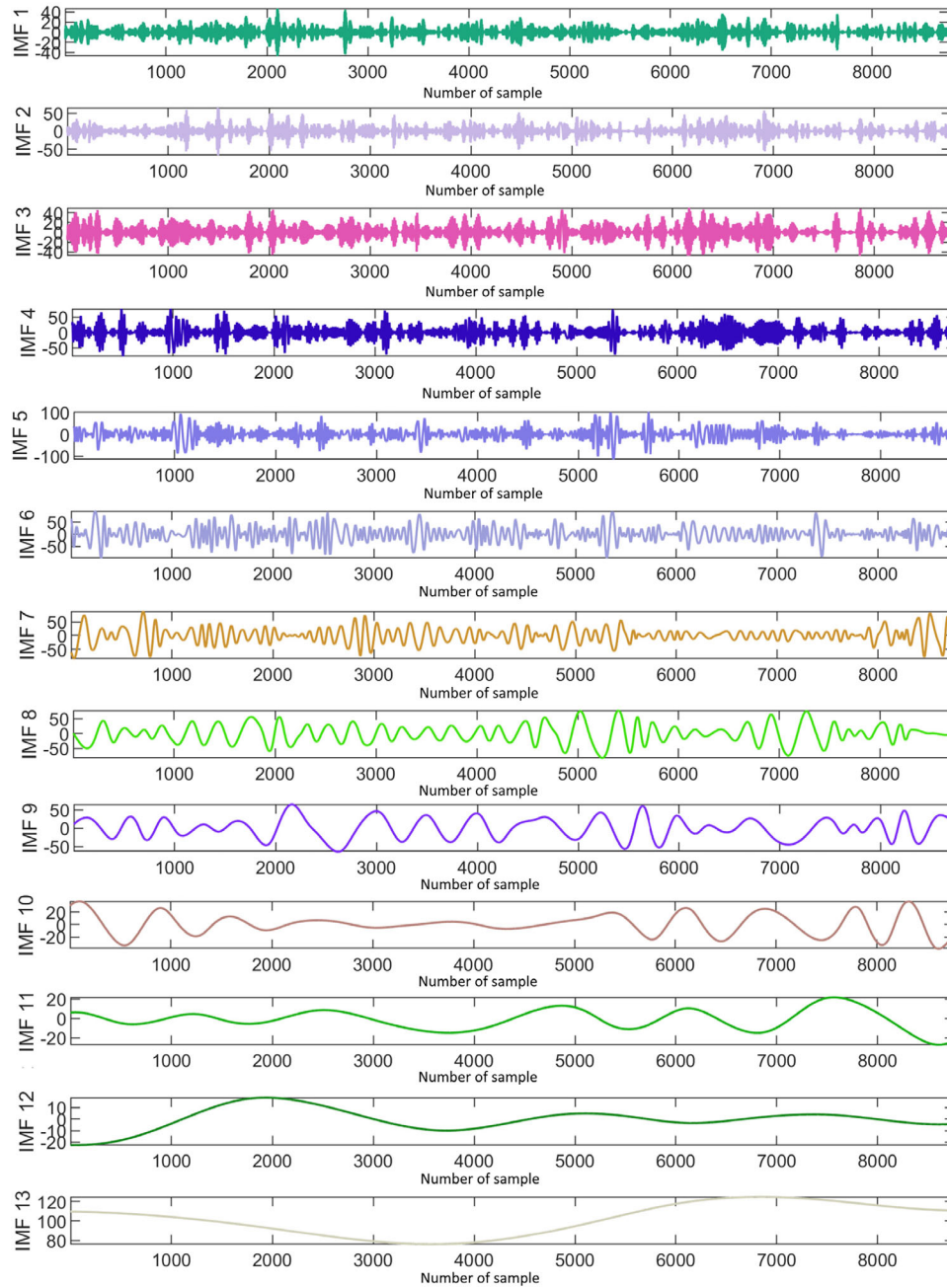


FIGURE 4 IMF signals decomposed by the EMD method for West of Duddon Sands OWF wind power dataset.

decomposition of the highest-frequency IMF signal. The utilization of the VMD method aimed to further decompose the highest-frequency IMF signal and extract more information. In the secondary decomposition process, an additional five IMF signals were obtained. A total of 17 IMF signals were obtained, comprising 12 signals from the first decomposition process excluding the highest frequency component IMF1, and five signals from the secondary decomposition of IMF1.

The decomposed IMF signals obtained are utilized as inputs to the LSTM model using the sliding window technique. In the sliding window technique, the window size is selected as three,

demonstrating that each LSTM model has three inputs. As each LSTM model is designed to predict the next step as an output, the model has one output. In summary, the 17 obtained IMF signals are first trained using the sliding window technique in LSTM models with three inputs and one output, using the same parameters, for 70% of the dataset. The number of LSTMs in the EVL model is equal to the number of IMF signals and each LSTM model forecasts the subsequent step of the primary and secondary decomposition signals in the output. The output values of 17 LSTMs are combined to predict the next step of wind power. During the training process, the LSTM model weights

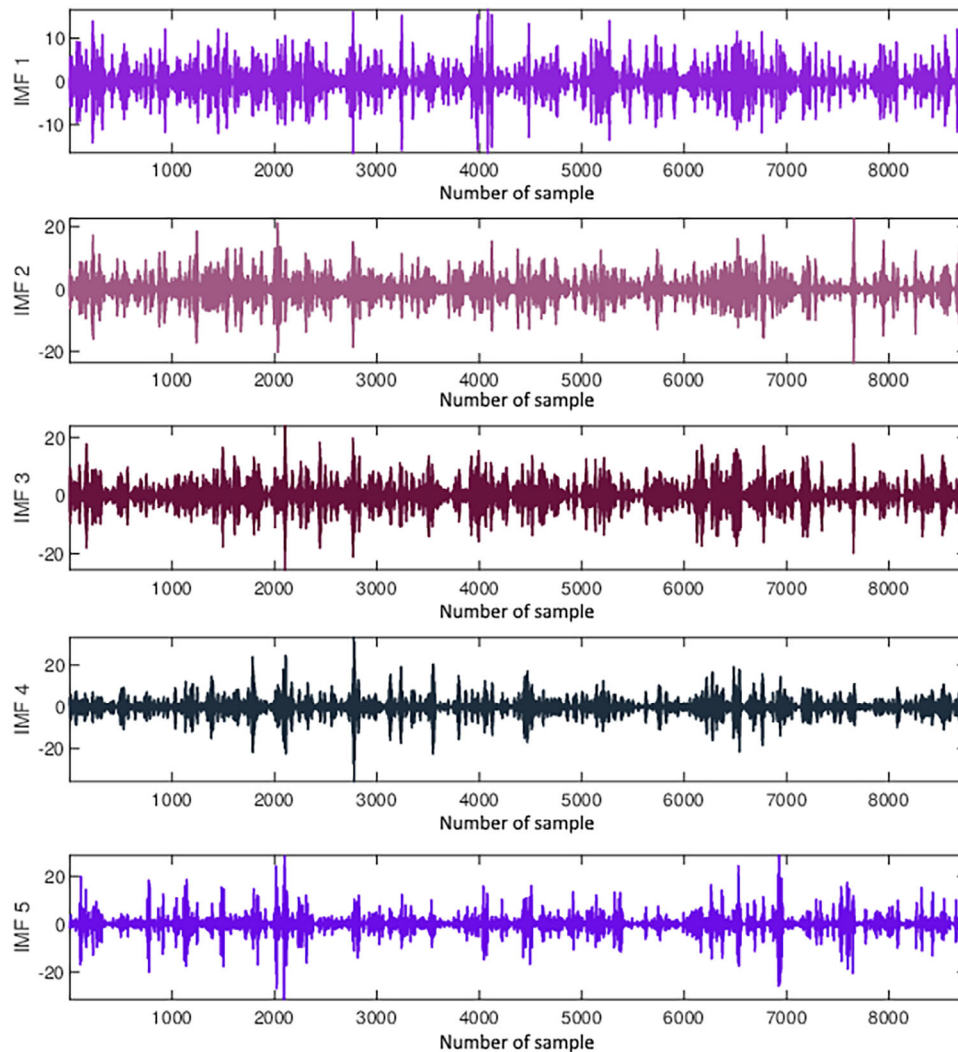


FIGURE 5 Secondary IMF signals decomposed by the VMD for West of Duddon Sands OWF wind power dataset.

were optimized by minimizing the mean squared error (MSE) metric using the Adam method. Figure 6 shows the training output results of each LSTM in the EVL model for West of Duddon Sands OWF dataset.

The performance of the EVL model for the West of Duddon Sands Dataset is shown in Figure 7. This figure is comprised of five subfigures, each illustrating different aspects of the results of the model. The top two subfigures depict the training and test results of the EVL model, respectively, whereas the last three subfigures demonstrate the error, error histogram, and scatter plots between the measured and estimated wind power during the training phase.

The results of the training and testing phases of the EVL model suggest that it has promising performance in predicting short-term wind power in the West of Duddon Sands OWF. Examination of the error distribution, for this dataset with the highest standard deviation, reveals that the error is evenly spread around zero. Furthermore, the scatter plot between the measured and forecasted wind power data for West of Duddon

Sands OWF displays a strong positive correlation, indicating the efficacy of the model in accurately predicting the actual wind power data during the training phase.

The training results of the EVL model applied to the Horns Power OWF wind data set obtained are presented in Figure 8. In this figure, the top figure displays the comparison of the short-term wind power forecasting results with the actual wind power data. The middle part shows the error values during the training, the histogram distribution of these error values, and the scatter plot between the measured and the forecasted values. In the last row, the comparison of the test results is presented.

It can be inferred from these figures that the EVL model performed successfully in estimating wind power during its training phase, as evidenced by the high correlation observed in the scatter plot and the uniform distribution of error around zero as demonstrated in the error histogram. However, the data between the hours of 6603 and 6801, within a 1-year segment of the data set, was recorded as zero due to various technical

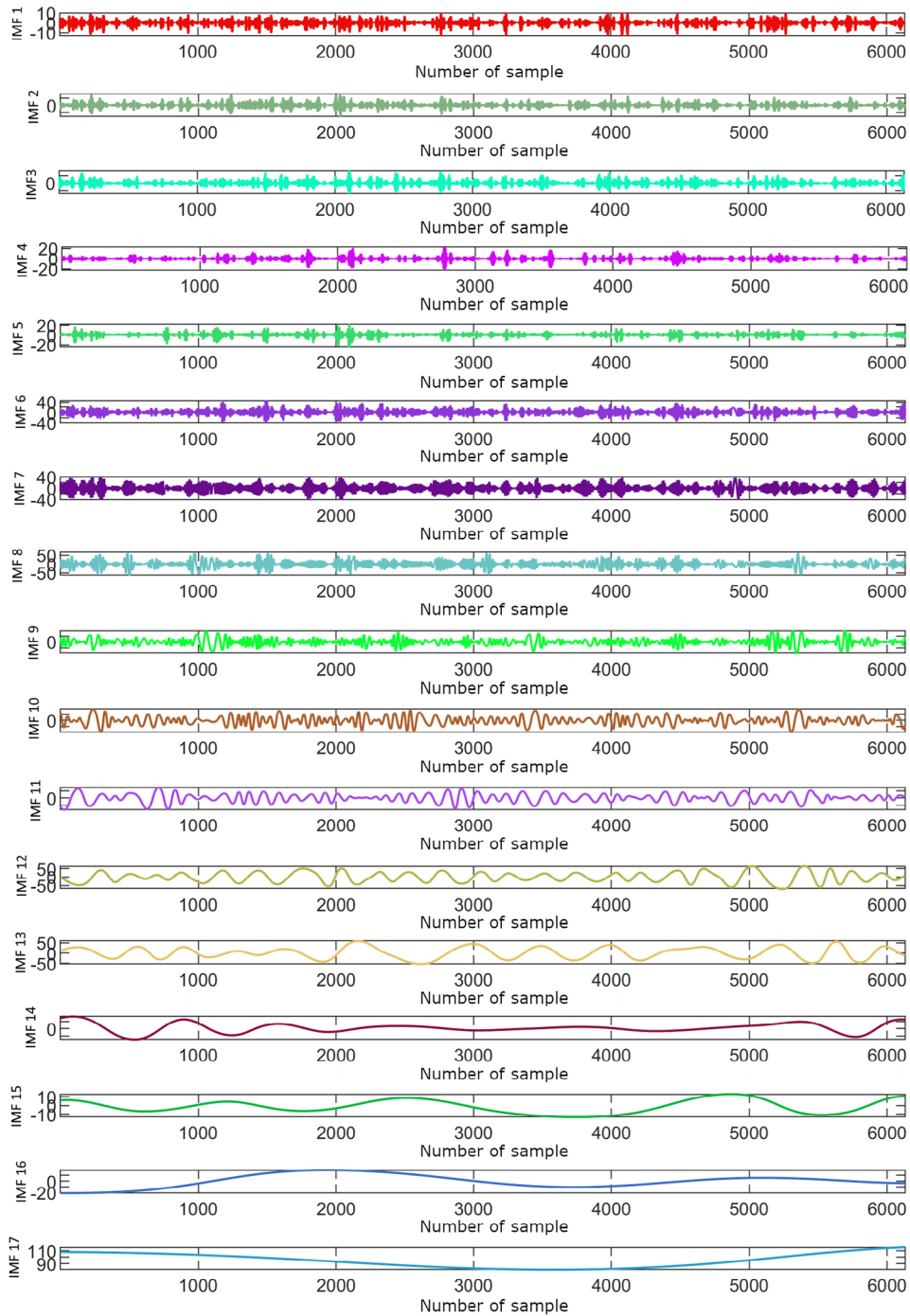


FIGURE 6 Training output results of the LSTMs in the EVL model for the West of Duddon Sands OWF dataset.

problems at the wind turbines during that period. Despite this, the original data was utilized in this analysis instead of removing the mentioned segment. As a result, while the actual value was zero during the mentioned interval, the EVL model's predictions exhibited fluctuations. Nonetheless, during the test time excluding this interval, the EVL model effectively estimated wind power for the Horns Power dataset.

Figure 9 shows the results for Barrow OWF dataset. As previously presented, the figure consists of five different sub-figures.

The top sub-figure depicts the results of the training process of the EVL model, demonstrating its ability to forecast wind power accurately. The first sub-figure in the second row depicts the error plot, showing a narrower range of variability compared to the other two data sets. The second sub-figure, the error histogram, shows that the error is evenly distributed between -10 and 10 . The final sub-figure provides the positive correlation between the measured and forecasted wind power data during the training stage. The sub-figures in the last row present the

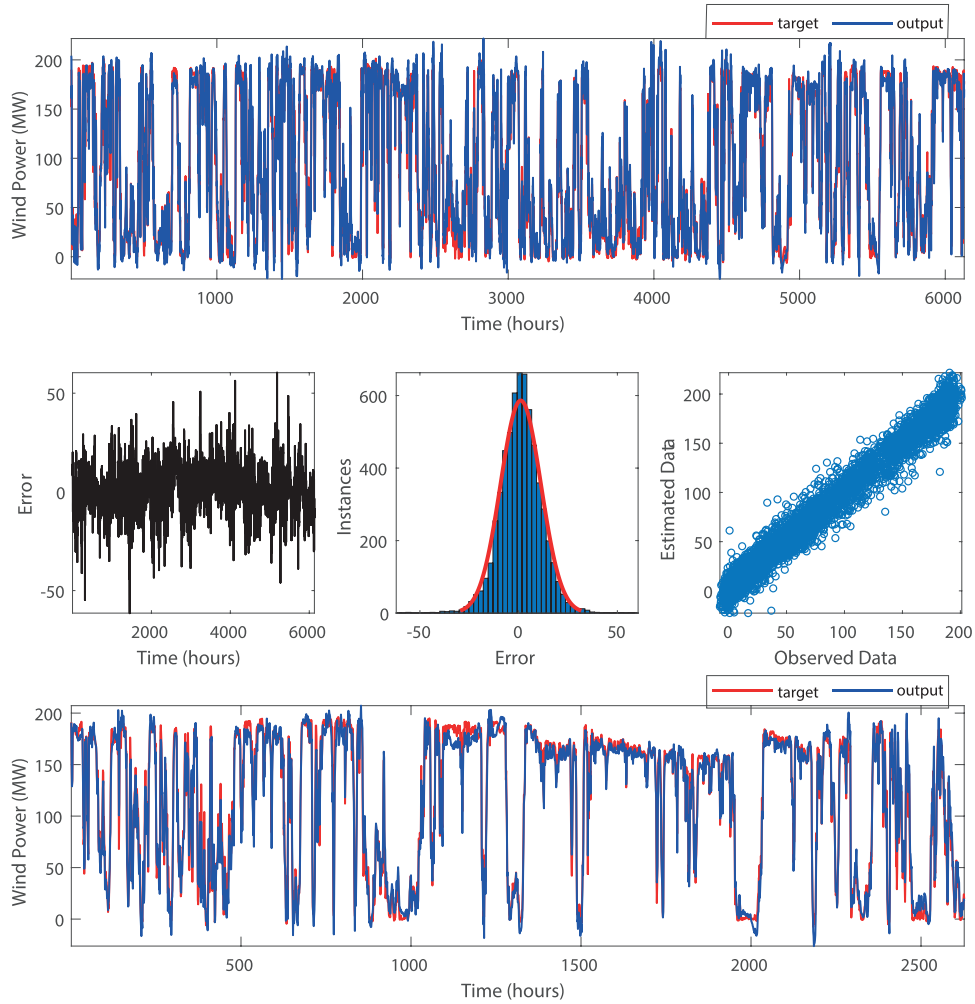


FIGURE 7 Training and test results of the EVL model for the West of Duddon Sands OWF wind dataset.

test results. It can be observed that the EVL model demonstrate close correlation with the actual wind power data for short-term wind power forecasting for different test data sets from the training set.

Five different time series forecasting models, including the standard LSTM, EMD-LSTM, EMD-WD-LSTM, and EMD-SWD-LSTM models, are used for comparison analysis. The hyperparameters of the LSTM model are kept constant across all models, and the EMD, the WD, and the SWD decomposition methods are applied in the preprocessing stage of real wind power data. The models were created without any decomposition method, with a single decomposition and multiple decomposition methods. The results of all the implemented models for West of Duddon Sands OWF are shown in Figure 10. It is observed that the proposed model results given in blue displays the best fit to the real data, while LSTM model results without the preprocessing step display the most inconsistency. It is clear that the decomposition step improved the forecasting performance. In the local zoomed-in plot, the single LSTM model had significant errors compared to the LSTM models with the decomposition methods. The reason for the

large error can be said that the single LSTM cannot forecast accurately for high-frequency components in the original signal. To overcome this issue, with the decomposition methods, the original signal is divided into sub-components. Then, all sub-signals are fed to the LSTM. While multiple decomposition with the SWD and VMD increase the model performance, the WD-based secondary decomposition does not provide sufficient results. The reason may be that WD does not capture of global frequency information of IMF_1 .

To quantify the impact of the secondary decomposition on the forecasting performance, four criteria were used. These are MSE, root mean squared error (RMSE), mean absolute error (MAE), and R-squared (R^2), which are calculated as follows:

$$RMSE = \sqrt{\frac{\sum_{i=1}^N (y_i - \tilde{y}_i)^2}{N}}, \quad (10)$$

$$MAE = \frac{1}{N} \sum_{i=1}^N |y_i - \tilde{y}_i|, \quad (11)$$

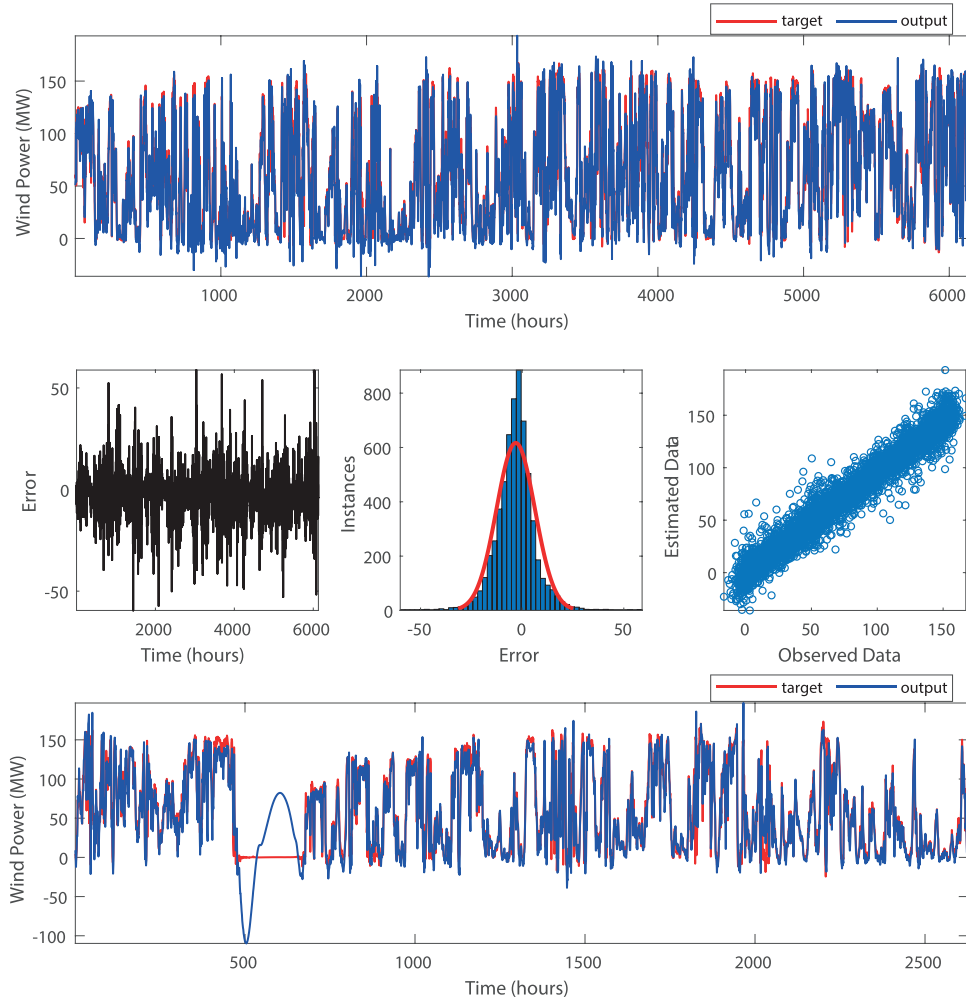


FIGURE 8 Training and test results of the EVL model for the Horns Power OWF wind dataset.

$$\text{MSE} = \frac{\sum_{i=1}^N (y_i - \tilde{y}_i)^2}{N}, \quad (12)$$

$$R^2 = 1 - \frac{\sum_{i=1}^N (y_i - \tilde{y}_i)^2}{\sum_{i=1}^N (y_i - \bar{y})^2}. \quad (13)$$

Herein, y_i and \tilde{y}_i are the actual and forecasted values, respectively. N indicates the number of samples. Performance metric analysis is a powerful tool to evaluate whether the model is effective and can perform the accuracy of the model's forecasting results. These metrics are selected to assess both the training and testing phases of each model. The results of the comparison analysis are reported in the tables below, with each metric serving as a means of evaluating the accuracy and robustness of the models. The comparison results for West of Duddon Sands OWF are summarized in Table 2.

In terms of performance metrics in Table 2, the proposed model outperforms with MSE, RMSE, MAE, and R^2 values of 96.154, 9.8058, 7.5288, and 0.9790, respectively, for the test phase. In terms of accuracy for the training phase, the perfor-

mance of the implemented models from the best to the worst can be sorted to be EMD-VMD-LSTM, EMD-SWD-LSTM, EMD-LSTM, EMD-WD-LSTM, and LSTM, with R^2 values of 0.9800, 0.9742, 0.9694, 0.9287, and 0.9249, respectively. It is observed that the use of the WD in secondary decomposition does not provide an advantage. Contrary to this, the SWD and VMD were found to increase the forecasting performance. The reason is that with the use of SWD and VMD for secondary decomposition, there is no critical data loss in IMF_1 original data, unlike the WD.

Similarly, Table 3 presents the results for the Horns Power OWF dataset. As can be seen from the table, the proposed EVL model achieved the lowest MSE, RMSE, and MAE values, and the highest R^2 value for training and test datasets. The reason of lower performance achieved in the test phase as compared to the training phase is that the OWF is not operational in a certain time period. This time interval is also clearly shown in Figure 8. Considering that the sliding windowing technique is used, the input data containing missing data during the test phase reduces the forecasting performance. Despite all this, the proposed model achieved R^2 value of 0.8556.

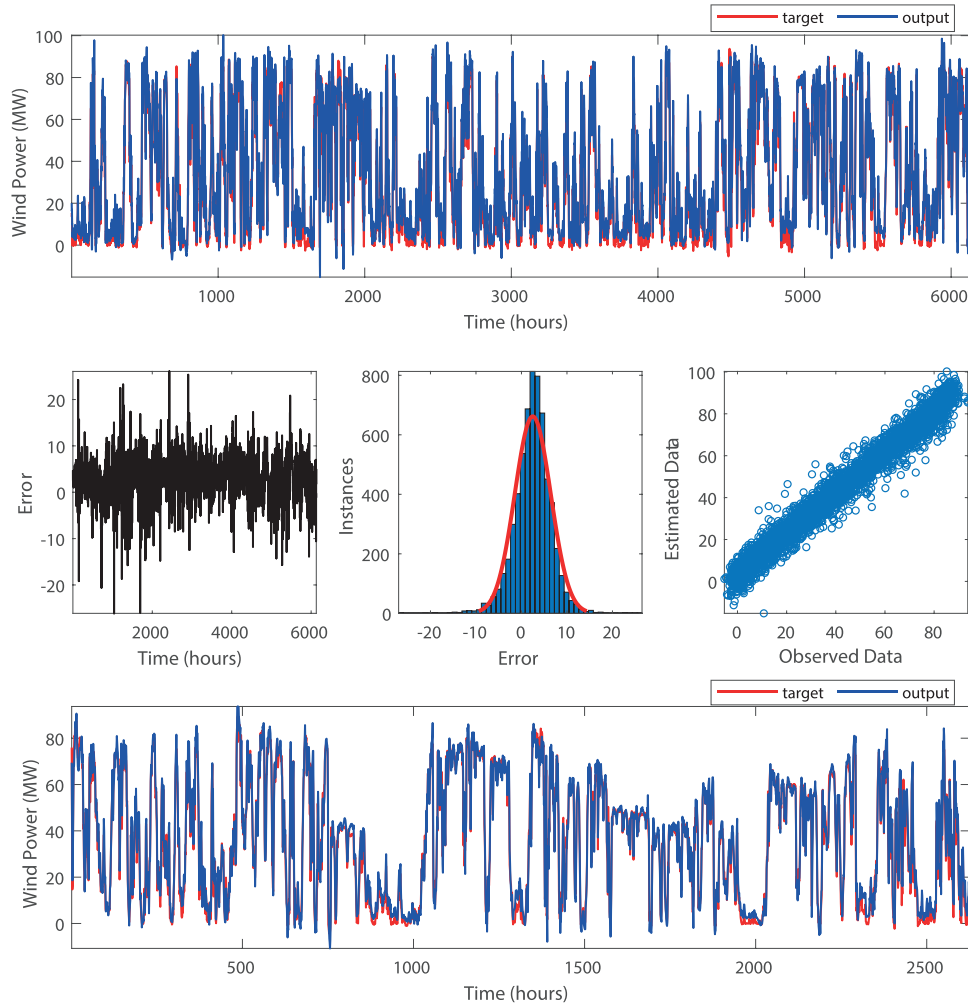


FIGURE 9 Training and test results of the EVL model for the Barrow OWF wind dataset.

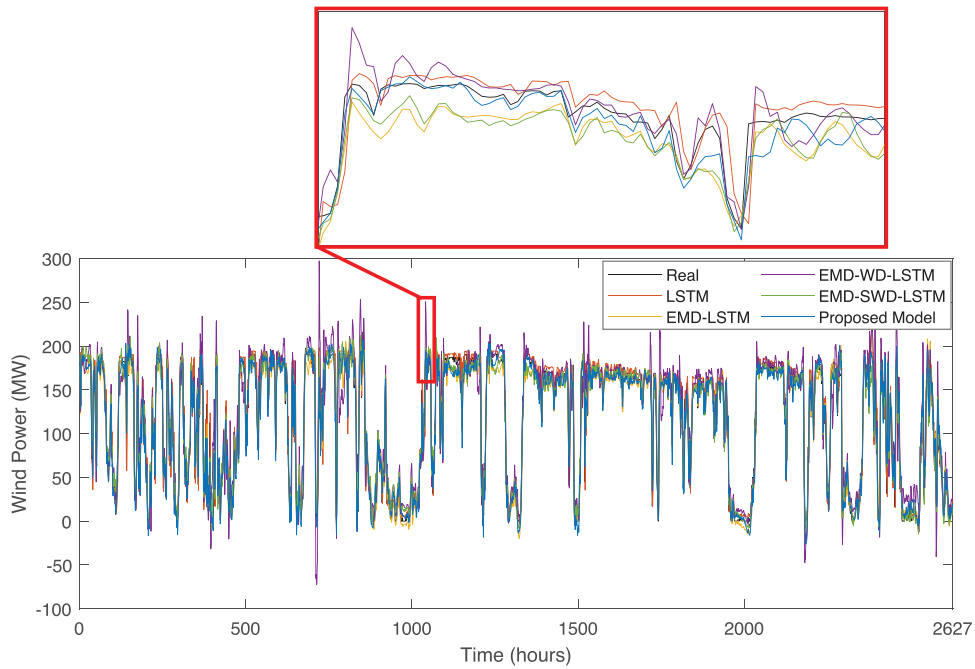


FIGURE 10 Comparison of the forecasting test results of the implemented models.

TABLE 2 The comparison results for West of Duddon Sands OWF wind power data.

Metric	LSTM		EMD		EMD-WD		EMD-SWD		EMD-VMDLSTM	
	LSTM									
	Training	Test	Training	Test	Training	Test	Training	Test	Training	Test
MSE	399.58	397.46	162.85	169.59	458.64	462.67	137.35	130.87	105.53	96.154
RMSE	19.99	19.936	12.761	13.023	21.416	21.51	11.72	11.44	10.273	9.8058
MAE	12.644	12.677	9.5021	9.9876	14.371	14.366	8.6473	8.5693	7.8572	7.5288
R^2	0.9249	0.9120	0.9694	0.9625	0.9287	0.9173	0.9742	0.9710	0.9800	0.9790

TABLE 3 The comparison results for Horns Power OWF wind power data.

Metric	LSTM		EMD		EMD-WD		EMD-SWD		EMD-VMD	
	LSTM									
	Training	Test	Training	Test	Training	Test	Training	Test	Training	Test
MSE	429.06	561.5	168.76	785.19	595.02	22735	145.94	666.92	99.171	382.91
RMSE	20.714	23.696	12.991	28.021	24.393	150.78	12.081	25.825	9.9584	19.568
MAE	12.636	13.644	9.0148	15.91	14.878	49.278	8.594	14.835	7.2677	11.434
R^2	0.8354	0.7863	0.9353	0.7013	0.8660	0.5448	0.9440	0.7463	0.9622	0.8556

TABLE 4 The comparison results for Barrow OWF wind power data.

Metric	LSTM		EMD		EMD-WD		EMD-SWD		EMD-VMD	
	LSTM		LSTM		LSTM		LSTM		LSTM	
	Training	Test	Training	Test	Training	Test	Training	Test	Training	Test
MSE	77.161	70.14	25.422	22.108	16.474	16.937	30.724	22.605	21.773	15.202
RMSE	8.7841	8.3749	5.042	4.7019	4.0588	4.1154	5.5429	4.7545	4.6662	3.899
MAE	5.8897	5.4376	3.7225	3.3991	3.0199	3.1368	4.3318	3.5406	3.7177	2.9694
R^2	0.9095	0.8912	0.9702	0.9657	0.9804	0.9737	0.9640	0.9649	0.9746	0.9766

For Barrow dataset, the comparison results are summarized in Table 4. The results show that among the models, the EVL model has the best performance on the test set in terms of all the metrics considered. For the training dataset, the EMD-WD-LSTM hybrid model has the best performance in terms of all metrics. The EVL model's training performance is the second rank. Therefore, both models display a competitive approach for the training and test phases.

To further assess the effectiveness of the proposed model, the Taylor diagrams are drawn as given in Figure 11. The Taylor diagram represents the root-mean-square deviation (RMSD), correlation coefficient, and standard deviation. In this respect, all the models can be compared on the basis of how well they forecast the target data. The square symbol in pink denotes the proposed EVL model. As can be seen, the proposed model has the lowest RMSD and standard deviation. Moreover, the correlation coefficient value is nearly 1 for all datasets. An analysis of

the results obtained from the three OWF wind power datasets indicates that the proposed EVL model demonstrates the most superior performance when compared to the other forecasting models employed in this study. Compared with other models, adding the VMD as a secondary decomposition method with the EMD can make full use of the input features and give clearer meaning to the features and forecasted wind power.

4 | CONCLUSION

This paper proposed a new forecasting model based on the LSTM neural network enhanced by multiple signal decomposition techniques. This model incorporated two stages of signal decomposition, namely, the EMD and VMD, within a deep learning-based LSTM framework. The motivation behind this research was to enhance forecasting accuracy by

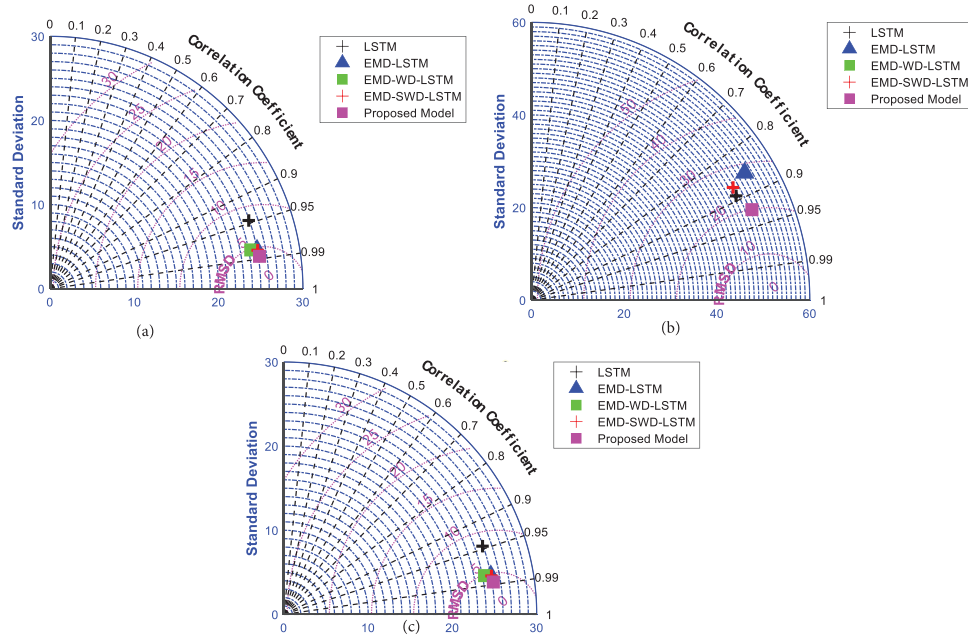


FIGURE 11 The Taylor diagrams of the forecasting models for (a) The West of Duddon Sands OWF, (b) Horns Power OWF, (c) Barrow OWF wind farm datasets.

addressing the intricate patterns within wind power signals. Recognizing the need for a secondary decomposition approach for the highest-frequency components, an effort was made to capture the diverse and dynamic nature of wind data. Testing of the proposed model was conducted using real wind power data obtained from three distinct OWFs. Subsequently, a comprehensive comparative analysis was performed with the EVL model against various LSTM models integrated with different signal decomposition techniques, including EMD-WD-LSTM, EMD-LSTM, EMD-SWD-LSTM, and the conventional LSTM model.

The findings revealed that the EVL model consistently outperformed the alternative models, demonstrating superior accuracy with lower error metrics and the highest R^2 value. As an example, when the Barrow OWF dataset is considered, it is observed that a 53.44% reduction in the RMSE value is achieved by the proposed model in comparison to a single model without any signal decomposition method. Furthermore, the proposed model achieved consistent reductions in RMSE ranging from 5.25% to 17.99% when compared to other LSTM models incorporating multiple decomposition methods, namely EMD-WD and EMD-SWD. This substantial reduction in RMSE underscores the superior predictive capabilities of the proposed model in capturing and forecasting wind power data, signifying a noteworthy advancement in wind power forecasting accuracy.

AUTHOR CONTRIBUTIONS

Mehmet Balci: Conceptualization of this study; methodology; software. **Emrah Dokur:** Data curation; writing—original draft preparation. **Ugur Yuzgec:** Data curation; writing—original draft preparation. **Nuh Erdogan:** Data curation; writing—original draft preparation.

CONFLICT OF INTEREST STATEMENT

The authors declare no conflicts of interest.

DATA AVAILABILITY STATEMENT

Data subject to third party restrictions.

ORCID

Mehmet Balci  <https://orcid.org/0000-0003-0086-5584>

Emrah Dokur  <https://orcid.org/0000-0002-4576-1941>

Ugur Yuzgec  <https://orcid.org/0000-0002-5364-6265>

Nuh Erdogan  <https://orcid.org/0000-0003-1621-2748>

REFERENCES

1. Dokur, E., Erdogan, N., Salari, M.E., Karakuzu, C., Murphy, J.: Offshore wind speed short-term forecasting based on a hybrid method: Swarm decomposition and meta-extreme learning machine. *Energy* 248, 123595 (2022)
2. GWEC: GWEC global wind report 2023. Global Wind Energy Council, https://gwec.net/wp-content/uploads/2023/03/GWR-2023_interactive.pdf. Accessed 27 March 2023
3. Zhang, Z., Chen, Y., Liu, X., Wang, W.: Two-stage robust security-constrained unit commitment model considering time autocorrelation of wind/load prediction error and outage contingency probability of units. *IEEE Access* 7, 25398–25408 (2019)
4. Chen, Y., Zhang, Z., Chen, H., Zheng, H.: Robust UC model based on multi-band uncertainty set considering the temporal correlation of wind/load prediction errors. *IET Gener. Transm. Distrib.* 14, 180–190 (2020)
5. De Freitas, N., Silva, M.d.S., Sakamoto, M.S.: Wind speed forecasting: a review. *Int. J. Eng. Res. Appl.* 8, 4–9 (2018)
6. Sideratos, G., Hatziaargyriou, N.D.: An advanced statistical method for wind power forecasting. *IEEE Trans. Power Syst.* 22, 258–265 (2007)
7. Rajagopalan, S., Santoso, S.: Wind power forecasting and error analysis using the autoregressive moving average modeling. In: 2009 IEEE power & energy society general meeting, pp. 1–6. IEEE, Piscataway, NJ (2009)

8. Singh, P.K., Singh, N., Negi, R.: Wind power forecasting using hybrid ARIMA-ANN technique. In: *Ambient Communications and Computer Systems: RACCCS-2018*, pp. 209–220. Springer, Cham (2019)
9. Zhang, W., Lin, Z., Liu, X.: Short-term offshore wind power forecasting-a hybrid model based on discrete wavelet transform (DWT), seasonal autoregressive integrated moving average (SARIMA), and deep-learning-based long short-term memory (LSTM). *Renewable Energy* 185, 611–628 (2022)
10. Mabel, M.C., Fernandez, E.: Analysis of wind power generation and prediction using ANN: a case study. *Renewable Energy* 33, 986–992 (2008)
11. Liu, Y., Wang, J.: Transfer learning based multi-layer extreme learning machine for probabilistic wind power forecasting. *Appl. Energy* 312, 118729 (2022)
12. Liu, J., Wang, X., Lu, Y.: A novel hybrid methodology for short-term wind power forecasting based on adaptive neuro-fuzzy inference system. *Renewable Energy* 103, 620–629 (2017)
13. Lian, L., He, K.: Wind power prediction based on wavelet denoising and improved slime mold algorithm optimized support vector machine. *Appl. Energy* 46, 866–885 (2022)
14. Han, L., Jing, H., Zhang, R., Gao, Z.: Wind power forecast based on improved long short term memory network. *Energy* 189, 116300 (2019)
15. Yildiz, C., Acikgoz, H., Korkmaz, D., Budak, U.: An improved residual-based convolutional neural network for very short-term wind power forecasting. *Energy Convers. Manage.* 228, 113731 (2021)
16. Parmaksiz, H., Yuzgec, U., Dokur, E., Erdogan, N.: Mutation based improved dragonfly optimization algorithm for a neuro-fuzzy system in short term wind speed forecasting. *Knowl.-Based Syst.* 268, 110472 (2023)
17. Liu, H., Yang, R., Wang, T., Zhang, L.: A hybrid neural network model for short-term wind speed forecasting based on decomposition, multi-learner ensemble, and adaptive multiple error corrections. *Renewable Energy* 165, 573–594 (2021)
18. Liu, M.D., Ding, L., Bai, Y.L.: Application of hybrid model based on empirical mode decomposition, novel recurrent neural networks and the ARIMA to wind speed prediction. *Energy Convers. Manage.* 233, 113917 (2021)
19. Liu, H., Mi, X., Li, Y., Duan, Z., Xu, Y.: Smart wind speed deep learning based multi-step forecasting model using singular spectrum analysis, convolutional gated recurrent unit network and support vector regression. *Renewable Energy* 143, 842–854 (2019)
20. Ou, Y., Xu, L., Wang, J., Fu, Y., Chai, Y.: A STL decomposition-based deep neural networks for offshore wind speed forecasting. *Appl. Energy* 46, 1753–1774 (2022)
21. Pradhan, P.P., Subudhi, B.: Wind speed forecasting based on wavelet transformation and recurrent neural network. *Int. J. Numer. Modell. Electron. Networks Devices Fields* 33, e2670 (2020)
22. Dokur, E., Erdogan, N., Kucuksari, S.: EV fleet charging load forecasting based on multiple decomposition with CEEMDAN and swarm decomposition. *IEEE Access* 10, 62330–62340 (2022)
23. Apostolidis, G.K., Hadjileontiadis, L.J.: Swarm decomposition: a novel signal analysis using swarm intelligence. *Signal Process.* 132, 40–50 (2017)
24. Qian, Z., Pei, Y., Zareipour, H., Chen, N.: A review and discussion of decomposition-based hybrid models for wind energy forecasting applications. *Appl. Energy* 235, 939–953 (2019)
25. Pillai, G.N., Shihabudheen, K.: Wind speed forecasting using empirical mode decomposition and regularized ELANFIS. In: *2017 IEEE Symposium Series on Computational Intelligence (SSCI)*, pp. 1–7. IEEE, Piscataway, NJ (2017)
26. Liu, H., Tian, H., Liang, X., Li, Y.: New wind speed forecasting approaches using fast ensemble empirical model decomposition, genetic algorithm, mind evolutionary algorithm and artificial neural networks. *Renewable Energy* 83, 1066–1075 (2015)
27. Liu, H., Mi, X., Li, Y.: Smart multi-step deep learning model for wind speed forecasting based on variational mode decomposition, singular spectrum analysis, LSTM network and ELM. *Energy Convers. Manage.* 159, 54–64 (2018)
28. Jiang, Z., Che, J., He, M., Yuan, F.: A CGRU multi-step wind speed forecasting model based on multi-label specific XGBoost feature selection and secondary decomposition. *Renewable Energy* 203, 802–827 (2023)
29. Wang, J., He, M., Qiu, S.: Two-stage decomposition multi-scale nonlinear ensemble model with error-correction-coupled Gaussian process for wind speed forecast. *Atmosphere* 14, 395 (2023)
30. Liu, B., Xie, Y., Wang, K., Yu, L., Zhou, Y., Lv, X.: Short-term multi-step wind direction prediction based on OVMD quadratic decomposition and LSTM. *Sustainability* 15, 11746 (2023)
31. Zhai, C., Li, H.: Short-term wind speed prediction based on quadratic decomposition improved particle swarm optimization extreme learning machine. In: *2022 9th International Forum on Electrical Engineering and Automation (IFEAA)*, pp. 1186–1191. IEEE, Piscataway, NJ (2022)
32. Emeksiz, C., Tan, M.: Multi-step wind speed forecasting and hurst analysis using novel hybrid secondary decomposition approach. *Energy* 238, 121764 (2022)
33. da Silva, R.G., Moreno, S.R., Ribeiro, M.H.D.M., Larcher, J.H.K., Mariani, V.C., dos Santos Coelho, L.: Multi-step short-term wind speed forecasting based on multi-stage decomposition coupled with stacking-ensemble learning approach. *Int. J. Electr. Power Energy Syst.* 143, 108504 (2022)
34. Sibtain, M., Bashir, H., Nawaz, M., Hameed, S., Azam, M.I., Li, X., et al.: A multivariate ultra-short-term wind speed forecasting model by employing multistage signal decomposition approaches and a deep learning network. *Energy Convers. Manage.* 263, 115703 (2022)
35. Zhang, Y., Zhang, W., Guo, Z., Zhang, S.: An effective wind speed prediction model combining secondary decomposition and regularised extreme learning machine optimised by cuckoo search algorithm. *Wind Energy* 25, 1406–1433 (2022)
36. Goh, H.H., He, R., Zhang, D., Liu, H., Dai, W., Lim, C.S., et al.: A multimodal approach to chaotic renewable energy prediction using meteorological and historical information. *Appl. Soft Comput.* 118, 108487 (2022)
37. Sun, H., et al.: Hybrid model with secondary decomposition, randomforest algorithm, clustering analysis and long short memory network principal computing for short-term wind power forecasting on multiple scales. *Energy* 221, 119848 (2021)
38. Sun, W., Tan, B., Wang, Q.: Multi-step wind speed forecasting based on secondary decomposition algorithm and optimized back propagation neural network. *Appl. Soft Comput.* 113, 107894 (2021)
39. Zhang, S., Chen, Y., Xiao, J., Zhang, W., Feng, R.: Hybrid wind speed forecasting model based on multivariate data secondary decomposition approach and deep learning algorithm with attention mechanism. *Renewable Energy* 174, 688–704 (2021)
40. Wu, Z., Xia, X., Xiao, L., Liu, Y.: Combined model with secondary decomposition-model selection and sample selection for multi-step wind power forecasting. *Appl. Energy* 261, 114345 (2020)
41. Xiang, L., Li, J., Hu, A., Zhang, Y.: Deterministic and probabilistic multi-step forecasting for short-term wind speed based on secondary decomposition and a deep learning method. *Energy Convers. Manage.* 220, 113098 (2020)
42. Wu, Z., Xiao, L.: A secondary decomposition based hybrid structure with meteorological analysis for deterministic and probabilistic wind speed forecasting. *Appl. Soft Comput.* 85, 105799 (2019)
43. Liu, H., Duan, Z., Wu, H., Li, Y., Dong, S.: Wind speed forecasting models based on data decomposition, feature selection and group method of data handling network. *Measurement* 148, 106971 (2019)
44. Zhang, Y., Chen, B., Pan, G., Zhao, Y.: A novel hybrid model based on VMD-WT and PCA-BP-RBF neural network for short-term wind speed forecasting. *Energy Convers. Manage.* 195, 180–197 (2019)
45. Liu, H., Duan, Z., Han, F., Li, Y.F.: Big multi-step wind speed forecasting model based on secondary decomposition, ensemble method and error correction algorithm. *Energy Convers. Manage.* 156, 525–541 (2018)
46. Zeiler, A., Faltermeier, R., Keck, I.R., Tomé, A.M., Puntonet, C.G., Lang, E.W.: Empirical mode decomposition-an introduction. In: *The 2010 International Joint Conference on Neural Networks (IJCNN)*, pp. 1–8. IEEE, Piscataway, NJ (2010)
47. Huang, N.E., Shen, Z., Long, S.R., Wu, M.C., Shih, H.H., Zheng, Q., et al.: The empirical mode decomposition and the hilbert spectrum for nonlinear and non-stationary time series analysis. *Proc. R. Soc. Lond., Ser. A* 454, 903–995 (1998)

48. Lahmiri, S.: A variational mode decomposition approach for analysis and forecasting of economic and financial time series. *Expert Syst. Appl.* 55, 268–273 (2016)
49. ur Rehman, N., Aftab, H.: Multivariate variational mode decomposition. *IEEE Trans. Signal Process.* 67, 6039–6052 (2019)
50. Dragomiretskiy, K., Zosso, D.: Variational mode decomposition. *IEEE Trans. Signal Process.* 62, 531–544 (2013)
51. Soğanlı, A., Arıkan, O.: Joint multi-emitter signal separation and angle of arrival estimation via variational mode decomposition. In: 2017 25th Signal Processing and Communications Applications Conference (SIU), pp. 1–4. IEEE, Piscataway, NJ (2017)
52. Hochreiter, S., Schmidhuber, J.: Long short-term memory. *Neural Comput.* 9, 1735–1780 (1997)
53. Altan, A., Karasu, S.: Ayrıştırma yöntemlerinin derin öğrenme algoritması ile tanımlanan rüzgâr hızı tahmin modeli başarımına etkisinin incelenmesi. *Avrupa Bilim ve Teknoloji Dergisi*, pp. 844–853. DergiPark, Turkey (2020)

How to cite this article: Balci, M., Dokur, E., Yuzgec, U., Erdogan, N.: Multiple decomposition-aided long short-term memory network for enhanced short-term wind power forecasting. *IET Renew. Power Gener.* 18, 331–347 (2024). <https://doi.org/10.1049/rpg2.12919>